MOF Films Hot Paper

Deutsche Ausgabe: DOI: 10.1002/ange.201601754
Internationale Ausgabe: DOI: 10.1002/anie.201601754

Direct Fabrication of Free-Standing MOF Superstructures with Desired Shapes by Micro-Confined Interfacial Synthesis

*Jin-Oh Kim[+], Kyoung-Ik Min[+], Hyunwoo Noh, Dong-Hwi Kim, Soo-Young Park, and Dong-Pyo Kim**

Abstract: *Recently, metal–organic frameworks (MOFs) with multifunctional pore chemistry have been intensively investigated for positioning the desired morphology at specific locations onto substrates for manufacturing devices. Herein, we develop a micro-confined interfacial synthesis (MIS) approach for fabrication of a variety of free-standing MOF superstructures with desired shapes. This approach for engineering MOFs provides three key features: 1) in situ synthesis of various free-standing MOF superstructures with controlled compositions, shape, and thickness using a mold membrane; 2) adding magnetic functionality into MOF superstructures by loading with Fe_3O_4 nanoparticles; 3) transferring the synthesized MOF superstructural array on to flat or curved surface of various substrates. The MIS route with versatile potential opens the door for a number of new perspectives in various applications.*

Metal–organic frameworks (MOFs) are a class of multifunctional porous materials which are composed of metal ions and organic ligands linked through coordination bonds, and possessing open framework structures with inherent high microporosities.[1] With their facile preparation, high porosity, and tunable architecture, great efforts have been devoted, in the last two decades, to the synthesis of new open architectures with distinctive properties.[1,2] Recently, intensive research efforts are focused on controlling the morphology for construction of zero- (0D), one- (1D), two- (2D), and three-dimensional (3D) superstructures composed of well-intergrown nanocrystals as building blocks on desired substrates for device applications, such as sensors, electronics, supercapacitors, and batteries.[3–7]

For full and broad utilization of MOFs, it is highly desirable to have the capability to fabricate a free-standing MOF superstructure formable in any desired shape and to transfer this shaped superstructure to any desired substrate. The bottom-up approaches reported, such as Langmuir–Blodgett deposition, layer-by-layer, liquid-phase epitaxy, or self-assembly monolayer method are often complex, time consuming, and the shaping of the MOF involves multistep procedures.[4] Usually a secondary growth reaction was necessary on the seed-deposited surface of the substrate. Thus, the extra steps of template removal or peeling from the substrate might be needed to collect the free-standing MOF structures with specific shape, which often damaged the MOFs, leading to defects.

Moreover, imparting functionality and heterogeneity to MOFs has not yet been fully exploited, with the use of inappropriate additives, such as binders for fragile crystalline MOFs that damage their pristine features.[7] Therefore, it is desirable to develop an innovative synthetic method to localize such coordination reactions within a desired space for structuring the free-standing MOF assemblies into films, membranes, or patterns. In particular, the transfer of the structured MOF features would facilitate the integration of MOFs into device fabrication for application systems.

A synthetic approach based on interfacial interactions between aqueous metallic solution and organic ligand solution has been utilized to grow thin MOF layers and hollow capsules.[8a] Further, the interfacial microfluidic processes allowed formation of a hollow fiber membrane[8b] and enzyme encapsulated bio-MOF hollow spheres.[8c] Inspired by the interfacial growth of MOF, herein, we develop a micro-confined interfacial synthesis (MIS) approach for fabrication of a variety of free-standing MOF superstructures with desired shapes. This approach for engineering MOFs provides three key features: 1) in situ synthesis of various free-standing MOF superstructures with control over shape and thickness with the help of a mold membrane; 2) introducing functionality into heterogeneous MOF superstructures by loading them with iron oxide nanoparticles (Fe_3O_4 NPs); 3) transferring the synthesized MOF superstructural array to any desired location on flat or curved surfaces of various substrates (Figure 1). The availability of the MIS route opens the door for a number of new perspectives for fascinating device fabrication.

To fabricate the free-standing MOF superstructures with desired shapes, we adopted the immiscible liquid–liquid interfacial approach by placing a mold membrane with

[*] J.-O. Kim,[+] Dr. K.-I. Min,[+] D.-H. Kim, Prof. Dr. D.-P. Kim
National Centre of Applied Microfluidic chemistry
Department of Chemical Engineering
POSTECH (Pohang University of Science and Technology)
Pohang, 790-784 (Republic of Korea)
E-mail: dpkim@postech.ac.kr
H. Noh
Department of Mechanical Engineering
POSTECH (Pohang University of Science and Technology)
Pohang, 790-784 (Republic of Korea)
Prof. Dr. S.-Y. Park
Polymeric Nanomaterials Laboratory
Department of Polymer Science & Engineering
School of Applied Chemical Engineering
Kyungpook National University (KNU)
Daegu, 41566 (Republic of Korea)
[+] These authors contributed equally to this work.

Supporting information for this article can be found under: http://dx.doi.org/10.1002/anie.201601754.

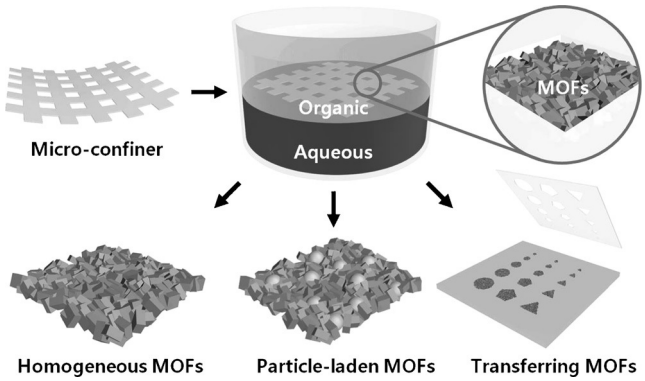

Figure 1. Schematic illustration of micro-confined interfacial synthesis capable of delivering MOF superstructures in homogeneous single phases (HKUST-1, ZIF-8, LnBTC), heterogeneous phases (particle-laden MOF), and subsequent transfer of the free-standing MOF patterns on various substrates.

desired shapes of open windows at the interface. An SU-8 mold as a micro-confiner could be suspended autonomously at the interface because of the density that is intermediate (896 $kg\,m^{-3}$) between water (997 $kg\,m^{-3}$, bottom) and 1-octanol (824 $kg\,m^{-3}$, top). The reliable interface positioning in the open window is crucial to the fabrication of the MOF superstructures with tunable thickness. The equilibrium position of the interface in the membrane mold is determined by the balance between two forces of buoyancy and capillarity. The depth H to which 1-octanol can penetrate into the mold window because of its better wettability of the polymer mold than water is given by the following relationship (for details, see Supporting Information S1) [Eq. (1)]:

$$H \leq \frac{4\gamma\cos\theta}{(\rho_{water}-\rho_{oil})gL} \quad (1)$$

where ρ is the density, g is the gravitational constant, γ is the surface tension, and θ is the angle of the interface. The force balance relation of [Eq. (1)] predicts that the liquid interface is positioned at the lowest point of the micro window as it was experimentally observed (Figure S1,S2). Therefore, the MIS system allows localization of the nucleation and growth via coordination reactions within the desired space in the open window of the micro-confiner.

For the purpose of generating various shapes of superstructures, the desired shapes with different dimensions in the range of approximately 100–500 μm in width and 50 μm in thickness were designed into the window arrays of the micro-confiner of SU-8 molds (40 × 40 mm). With the mold, the MIS process was carried out to fabricate various superstructures of HKUST-1, ZIF-8, and luminescent lanthanide MOF (LnBTC). In general, the micro-confiner is first floated on the surface of aqueous metal precursor solution, and then the organic ligand in 1-octanol with a deprotonation additive tributylamine is carefully introduced to form the desired interface array (Figure S3). The relatively high concentration of MOF precursors allowed rapid formation of MOF layers to fill up the windows within about 10 min (Movie S1). The selectively synthesized MOF superstructures were easily peeled off from the micro-confiner by gentle shaking.

Figure 2 shows the free-standing MOF superstructures of various shapes fabricated by the MIS process, including rectangle, circle, clover, star, heart, and even characters. The X-ray diffraction (XRD) of the fabricated MOFs (HKUST-1, ZIF-8, and LnBTC) confirmed that the superstructures consisted of uniformly phase-pure crystals (Figure S4,S5). In the case of HKUST-1, the Brunauer-Emmett-Teller (BET) surface area of 677 m^2g^{-1} was similar to the surface area of 620 m^2g^{-1} for the hollow MOF microspheres synthesized by the reported droplet interfacial method (Figure S6).[8a] The results are a demonstration that the micro-confiner can provide individually independent shape of spaces for MOF formation with no merged MOF superstructures. Moreover, the MOF superstructures synthesized by the MIS are shown to have good pattern fidelity and can be produced at a high rate of around 10^3 pieces per single batch of 10 min reaction (Figure 2 f). Heterolanthanide MOFs were also prepared by the MIS. The results show that the color of LnBTC can be tuned by controlling the ratio of Eu^{3+}, Ce^{3+}, and Tb^{3+} ions.[9]

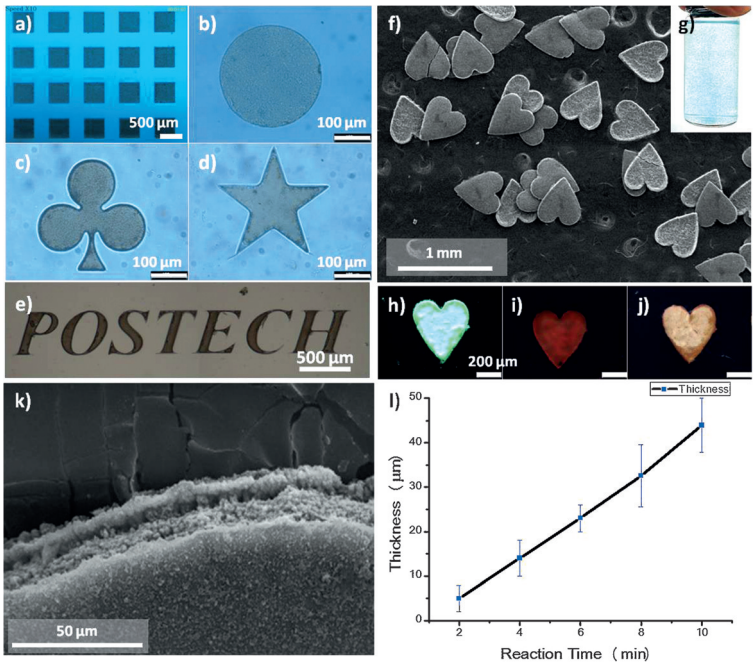

Figure 2. a)–e) Photographic images of various HKUST-1 superstructures (rectangle, circle, clover, star, and characters "POSTECH") grown in the micro-confiner. f) SEM image of heart-shaped MOF superstructures removed from the mold after reaction time of 10 min and g) photographic image of dispersed superstructures in the water, obtained by a single batch of MIS process (ca. 10^3 pieces per batch). h)–j) Photographs of luminescent lanthanide MOF (LnBTC) superstructures under exposure of UV light with wavelength of 265 nm; h) green TbBTC, i) red EuBTC, j) apricot heterolanthanide MOF (Eu:Ce:Tb = 25:20:55). k) SEM image of the layered edge of as-synthesized MOF superstructure. l) Reaction-time-dependent thickness control of HKUST-1 obtained from a 3D profiler.

The MOF superstructures show green (Tb), red (Eu), and apricot (Eu%:Ce%:Tb% of 25:20:55), respectively (Figure 2h–j).

To demonstrate the generality of the MIS, the approach was utilized for the fabrication of free-standing polypyrrole films.[10] As shown in Figure S7, circular polypyrrole films of different size (ca. 100–500 μm diameter, 30 μm thickness) were successfully synthesized by the reaction at the interface between water and cyclohexane for 30 min. This finding is an indication that the MIS can be used as a general platform for the formation of superstructures of various materials.

The process of the synthesized MOF filling up the open window of the mold can be inferred from the cross-sectional image at the edge of the superstructure that is given in Figure 2k, where the presence of stacked MOF layers is shown. A postulated explanation for this formation of the stacked layer is schematically illustrated in Figure S8. Initially, a layer of MOF forms at the bottom of the window where the water–organic interface exists. The aqueous precursor then penetrates through the gap between the mold wall and the first MOF crystal layer, re-establishing the reactive interface on top of the first MOF layer. It is likely that the resistive wetting of the penetrating aqueous precursor in the organic medium causes a burst overspreading on the MOF layer in several μm thickness, and the presence of organic ligand reagents in a sufficient amount at the top surface of the aqueous solution gave rise to a rapid nucleation-growth for the formation of a new dense MOF layer.[11] In addition, the aqueous precursor could also slowly permeate upward by soaking into the hydrophilic pores and vacancy of sparse MOF framework structure, which led to an irregular and slow nucleation-growth cycle under insufficient supply of counterpart reagent due to blocking by the dense top layer. Eventually, these two types of continuous growth cycle allowed the layered MOF superstructure with a periodic cross-sectional morphology. Similarly, the retarded permeation of the low-wetting organic-ligand solution downward to the bottom side of the MOF led to a rough morphology of the bottom surface, in contrast to a smooth surface at the top (Figure 2e and Figure S9). Consequently, the MOF layers would be gradually stacked up from the bottom of the window to reach several tens of micrometers in thickness with fast reaction time (ca. 10 min) in a linear time-dependent manner (Figure 2l). These results revealed that the MIS approach is facile and highly non-invasive for generating free-standing two-dimensional (2D) pattern structures for desired shape and size, in contrast to the reported 2D structuring methods where a polymer mixture or secondary growth is involved in the removal of the used templates.[4]

To demonstrate that functionality can be endowed on MOF superstructures, an MOF superstructure laden with Fe_3O_4 NPs (Fe_3O_4@HKUST-1) was successfully fabricated by homogeneously precipitating the pre-dispersed Fe_3O_4 NPs into the grown MOF interlayers (Figure 3). The particles are randomly distributed in the MOF as seen in the TEM image of Figure S11. However, when an external magnetic field was applied by placing the magnet at one side of the micro-confiner in the Petri dish, the precipitated Fe_3O_4 NPs were forced to become aligned along the direction of the magnetic field (Figure 3c,d and Figure S12).[12] Interestingly, the magnetically aligned Fe_3O_4@HKUST-1MOF rectangle enables motion actuation, such as rotation by controlling the direction of the applied external magnetic field (Figure 3e,f and Movie S2). Note that the magnet-responsive NPs-laden MOF superstructures provide unique capabilities, such as a non-invasive approach to remote control.[13]

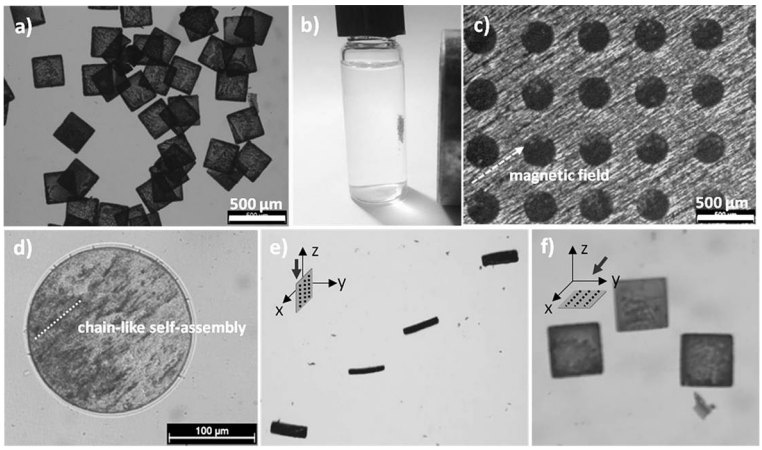

Figure 3. Free-standing functional MOF superstructures obtained by loading with magnetic nanoparticles (NPs). a,b) Optical images of Fe_3O_4@HKUST-1 rectangular superstructure. c,d) Optical images of MOF with Fe_3O_4 NPs of average size of 12 ± 7 nm across the circular windows aligned in the direction of the applied magnetic field during MIS process. e,f) Optical images on two types of actuating motions by Fe_3O_4@HKUST-1 rectangular superstructures, dependent of mutual direction between the aligned Fe_3O_4 NPs and the external magnetic field (thick black arrows).

The free-standing MOF superstructures of desired shape become useful when they are able to be placed on the wanted surfaces or substrates. This spatial positioning of various MOF patterns could be demonstrated by transferring the synthesized MOF superstructural array to the desired location. To promote adhesion of the transferred MOF patterns, polydopamine and silk fibroin were used that are known to easily bind with metal ions by coordination bond.[14] Prior to the contact transfer of MOF array patterns, the substrates such as glass and polyimide film were modified with polydopamine while the label of beaker, paper, and skin surface by silk fibroin (for detailed method see Supporting Information S2.8–10).[15] The MOF superstructural arrays on the SU-8 mold were successfully positioned onto various substrates (Figure 4). Moreover, a character pattern, such as "CAMC" composed of dots of MOF, was transferred on the curved surface of a glass vial to demonstrate the versatile positioning capability (Figure 4a,b). Further, the biocompatible ZIF-8 squares (300x 300×30 μm) array was transferred on the silk fibroin modified skin of hand with reliable adhesion and flexibility, which would be potentially useful for biomedical applications (Figure 4j,k). These results revealed that the transfer of MOF patterns prepared by MIS can easily be accomplished for broad selection of substrates of target

applications. It should be pointed out that the direct transfer of various MOF patterns with controlled shape and size is demonstrated on diverse substrates for the first time, which is compatible with multi-components systems. Therefore, this MIS approach allowing simple positioning of the functional MOF superstructures as desired enables to be utilized for fascinating device applications.

In summary, the interfacial MOF synthesis in the micro-confiner is a new strategy for preparing MOF superstructures by precisely controlling the morphology and the size in the 10^0–10^2 micron range. The free-standing MOF superstructures synthesized by the scalable MIS process were also functionalized by loading with magnetic nanoparticles and preparing luminescent heterolanthanide MOFs. Furthermore, the MOF superstructures can easily be contact-transferred to position the crystalline MOF superstructures on various substrates. This facile and versatile platform coupled with current electronic fabrication techniques is expected to open the way to the development of novel device applications.

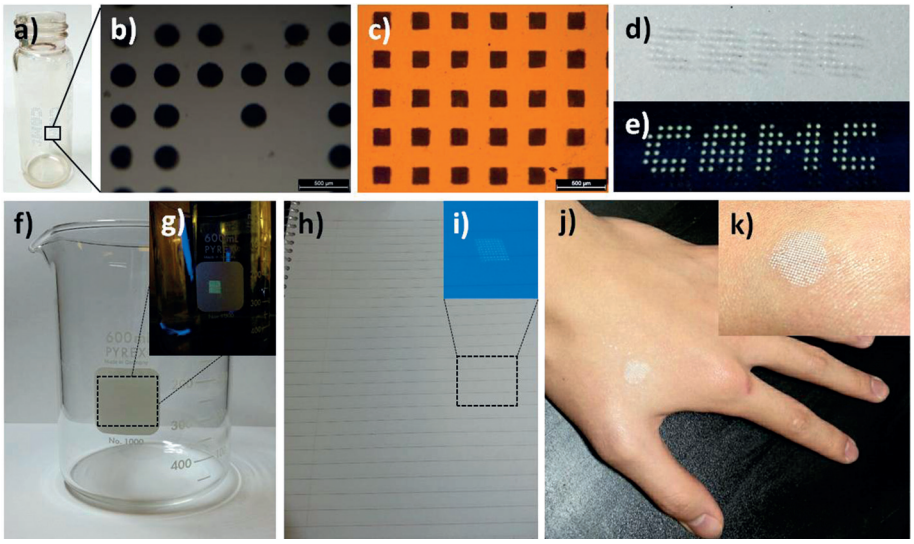

Figure 4. Transferring MOF superstructures onto various substrates (polyimide, glass, paper, skin). a,b) Photographs of transferred HKUST-1 dot (300 μm diameter) array for letter M on curved surface of glass vial. c) Photograph of transferred HKUST-1 square (200×200 μm) array pattern on polyimide film. d)–g) Photographs of transferred luminescent Tb-MOF array on d),e) glass substrate, f),g) white label of beaker, h),i) paper under day light and UV irradiation, respectively. j),k) Photographs of transferred ZIF-8 1 square (200 μm length) array on hand skin. The surfaces of glass vial and polyimide were pre-treated by polydopamine, whereas the white label of the beaker, paper, and skin were pre-coated with silk fibroin to promote adhesion of the transferred MOF patterns.

Acknowledgements

This work was supported by a National Research Foundation of Korea (NRF) grant funded by the Korean government (MSIP) (No.2008–0061983). We thank Dong-Hyeon Ko and Guan-Young Jeong for their technical support in preparation of this work.

Keywords: free-standing MOFs · interfacial synthesis · lanthanides · metal–organic frameworks · transfer

How to cite: *Angew. Chem. Int. Ed.* **2016**, *55*, 7116–7120
Angew. Chem. **2016**, *128*, 7232–7236

[1] a) H. Li, M. Eddaoudi, M. O'Keeffe, O. M. Yaghi, *Nature* **1999**, *402*, 276; b) N. Stock, S. Biswas, *Chem. Rev.* **2012**, *112*, 933–969; c) H. Furukawa, K. E. Cordova, M. O'Keeffe, O. M. Yaghi, *Science* **2013**, *341*, 1230444.

[2] a) J. S. Seo, D. Whang, H. Lee, S. I. Jun, J. Oh, Y. J. Jeon, K. Kim, *Nature* **2000**, *404*, 982; b) M. Eddaoudi, J. Kim, N. Rosi, D. Vodak, J. Wachter, M. O'Keeffe, O. M. Yaghi, *Science* **2002**, *295*, 469; c) N. L. Rosi, J. Eckert, M. Eddaoudi, D. T. Vodak, J. Kim, M. O'Keeffe, O. M. Yaghi, *Science* **2003**, *300*, 1127; d) L. Pan, D. H. Olson, L. R. Ciemnolonski, R. Heddy, J. Li, *Angew. Chem. Int. Ed.* **2006**, *45*, 616; *Angew. Chem.* **2006**, *118*, 632; e) J. Lee, O. K. Farha, J. Roberts, K. A. Scheidt, S. T. Nguyen, J. T. Hupp, *Chem. Soc. Rev.* **2009**, *38*, 1450; f) R. J. Kuppler, D. J. Timmons, Q.-R. Fang, J.-R. Li, T. A. Makal, M. D. Young, D. Yuan, D. Zhao, W. Zhuang, H.-C. Zhou, *Coord. Chem. Rev.* **2009**, *253*, 3042; g) L. Song, J. Zhang, L. Sun, F. Xu, F. Li, H. Zhang, X. Si, C. Jiao, Z. Li, S. Liu, Y. Liu, H. Zhou, D. Sun, Y. Du, Z. Cao, Z. Gabelica, *Energy Environ. Sci.* **2012**, *5*, 7508; h) S. Chaemchuen, N. A. Kabir, K. Zhou, F. Verpoort, *Chem. Soc. Rev.* **2013**, *42*, 9304; i) T. Zhang, W. Lin, *Chem. Soc. Rev.* **2014**, *43*, 5982; j) P. Silva, S. M. F. Vilela, J. P. C. Tomé, F. A. A. Paz, *Chem. Soc. Rev.* **2015**, *44*, 6774.

[3] a) S. Furukawa, J. Reboul, S. Diring, K. Sumida, S. Kitagawa, *Chem. Soc. Rev.* **2014**, *43*, 5700; b) P. Falcaro, R. Ricco, C. M. Doherty, K. Liang, A. J. Hill, M. J. Styles, *Chem. Soc. Rev.* **2014**, *43*, 5513; c) V. Stavila, A. A. Talin, M. D. Allendorf, *Chem. Soc. Rev.* **2014**, *43*, 5994; d) D. Bradshaw, A. Garai, J. Huo, *Chem. Soc. Rev.* **2012**, *41*, 2344; e) L. E. Kreno, K. Leong, O. K. Farha, M. Allendorf, R. P. Van Duyne, J. T. Hupp, *Chem. Rev.* **2012**, *112*, 1105; f) M. D. Allendorf, A. Schwartzberg, V. Stavila, A. A. Talin, *Chem. Eur. J.* **2011**, *17*, 11372.

[4] a) S. Hermes, F. Schörder, R. Chelmowski, C. Wöll, R. A. Fischer, *J. Am. Chem. Soc.* **2005**, *127*, 13744; b) P. Falcaro, A. J. Hill, K. M. Nairn, J. Jasieniak, J. I. Mardel, T. J. Bastow, S. C. Mayo, M. Gimona, D. Gomez, H. J. Whitfield, R. Riccò, A. Patelli, B. Marmiroli, H. Amenitsch, T. Colson, L. Villanova, D. Buso, *Nat. Commun.* **2011**, *2*, 237; c) G. Lu, O. K. Farha, W. Zhang, F. Huo, J. T. Hupp, *Adv. Mater.* **2012**, *24*, 3970; d) K. Liang, C. Carbonell, M. J. Styles, R. Ricco, J. Cui, J. J. Richardson, D. Maspoch, F. Caruso, P. Falcaro, *Adv. Mater.* **2015**, DOI: 10.1002/adma.201503167; e) L. Pan, Z. Ji, X. Yi, X. Zhu, X. Chen, J. Shang, G. Liu, R.-W. Li, *Adv. Funct. Mater.* **2015**, *25*, 2677; f) E. Zanchetta, L. Malfatti, R. Ricco, M. J. Styles, F. Lisi, C. J. Coghlan, C. J. Doonan, A. J. Hill, G. Brusatin, P. Falcaro, *Chem. Mater.* **2015**, *27*, 690.

[5] a) R. Ameloot, L. Stappers, J. Fransaer, L. Alaerts, B. F. Sels, D. E. De Vos, *Chem. Mater.* **2009**, *21*, 2580; b) R. Ameloot, L. Pandey, M. Van der Auweraer, L. Alaerts, B. F. Selsa, D. E. De Vos, *Chem. Commun.* **2010**, *46*, 3735; c) I. Hod, W. Bury, D. M. Karlin, P. Deria, C.-W. Kung, M. J. Katz, M. So, B. Klahr, D. Jin, Y.-W. Chung, T. W. Odom, O. K. Farha, J. T. Hupp, *Adv. Mater.* **2014**, *26*, 6295.

[6] a) Y. Mao, J. Li, W. Cao, Y. Ying, P. Hu, Y. Liu, L. Sun, H. Wang, C. Jin, X. Peng, *Nat. Commun.* **2014**, *5*, 5532; b) K. Okada, R. Ricco, Y. Tokudome, M. J. Styles, A. J. Hill, M. Takahashi, P. Falcaro, *Adv. Funct. Mater.* **2014**, *24*, 1969; c) Y. Mao, L. shi, H. Huang, W. Cao, J. Li, L. Sun, X. Jina, X. Peng, *Chem. Commun.* **2013**, *49*, 5666; d) T. Toyao, K. Liang, K. Okada, R. Ricco, M. J. Styles, Y. Tokudome, Y. Horiuchi, A. J. Hill, M. Takahashi, M. Matsuoka, P. Falcaro, *Inorg. Chem. Front.* **2015**, *2*, 434.

[7] a) M. S. Denny Jr, S. M. Cohen, *Angew. Chem. Int. Ed.* **2015**, *54*, 9029; *Angew. Chem.* **2015**, *127*, 9157; b) A. K. Chaudhari, I. Han, J.-C. Tan, *Adv. Mater.* **2015**, *27*, 4438; c) B. Wu, J. Pan, L. Ge, L. Wu, H. Wang, T. Xu, *Sci. Rep.* **2014**, *4*, 4334; d) Y. Wu, F. Li, H. Liu, W. Zhu, M. Teng, Y. Jiang, W. Li, D. Xu, D. He, P. Hannam, G. Li, *J. Mater. Chem.* **2012**, *22*, 16971; e) R. Ostermann, J. Cravillon, C. Weidmann, M. Wiebcke, B. M. Smarsly, *Chem. Commun.* **2011**, *47*, 442.

[8] a) R. Ameloot, F. Vermoortele, W. Vanhove, M. B. J. Roeffaers, B. F. Sels, D. E. De Vos, *Nat. Chem.* **2011**, *3*, 382, b) A. J. Brown, N. A. Brunelli, K. Eum, F. Rashidi, J. R. Johnson, W. J. Koros, C. W. Jones, S. Nair, *Science* **2014**, *345*, 72; c) G.-Y. Jeong, R. Ricco, K. Liang, J. Ludwig, J.-O. Kim, P. Falcaro, D.-P. Kim, *Chem. Mater.* **2015**, *27*, 7903.

[9] a) Z. Hu, B. J. Deibert, J. Li, *Chem. Soc. Rev.* **2014**, *43*, 5815; b) Y. Cui, Y. Yue, G. Qian, B. Chen, *Chem. Rev.* **2012**, *112*, 1126; c) M. D. Allendorf, C. A. Bauer, R. K. Bhakta, R. J. T. Houk, *Chem. Soc. Rev.* **2009**, *38*, 1330.

[10] a) Q. Yang, Z. Hou, T. Huang, *J. Appl. Polym. Sci.* **2015**, *132*, 41615; b) G. Qi, Z. Wub, H. Wang, *J. Mater. Chem. C* **2013**, *1*, 7102.

[11] a) J. A. Greathouse, M. D. Allendorf, *J. Am. Chem. Soc.* **2006**, *128*, 10678; b) J. J. Low, A. I. Benin, P. Jakubczak, J. F. Abrahamian, S. A. Faheem, R. R. Willis, *J. Am. Chem. Soc.* **2009**, *131*, 15834; c) J. G. Nguyen, S. M. Cohen, *J. Am. Chem. Soc.* **2010**, *132*, 4560; d) E. S. Sanil, K.-H. Cho, D.-Y. Hong, J. S. Lee, S.-K. Lee, S. G. Ryu, H. W. Lee, J.-S. Chang, Y. K. Hwang, *Chem. Commun.* **2015**, *51*, 8418.

[12] a) J. Kim, S. E. Chung, S.-E. Choi, H. Lee, J. Kim, S. Kwon, *Nat. Mater.* **2011**, *10*, 747; b) H. Lee, J. Kim, H. Kim, J. Kim, S. Kwon, *Nat. Mater.* **2010**, *9*, 745.

[13] J. Thévenot, H. Oliveira, O. Sandre, S. Lecommandoux, *Chem. Soc. Rev.* **2013**, *42*, 7099.

[14] a) Y. Liu, K. Ai, L. Lu, *Chem. Rev.* **2014**, *114*, 5057; b) M. Zhou, J. Li, M. Zhang, H. Wang, Y. Lan, Y. Wu, F. Li, G. Li, *Chem. Commun.* **2015**, *51*, 2706; c) A. R. Abbasi, K. Akhbari, A. Morsali, *Ultrason. Sonochem.* **2012**, *19*, 846; d) Q. Dong, H. Su, D. Zhang, *J. Phys. Chem. B* **2005**, *109*, 17429.

[15] a) H. Lee, S. M. Dellatore, W. M. Miller, P. B. Messersmith, *Science* **2007**, *318*, 426; b) D. N. Rockwood, R. C. Preda, T. Yücel, X. Wang, M. L. Lovett, D. L. Kaplan, *Nat. Protoc.* **2011**, *6*, 1612.

Received: February 19, 2016
Published online: May 3, 2016

